Spectral emission analysis of a dc helium hollow cathode discharge

O. H. Chin and C. S. Wong
Plasma Research Laboratory, Physics Department, University of Malaya, 50603 Kuala Lumpur, Malaysia

(Received 21 December 2002)

A fully developed hollow cathode discharge in which the negative glows from opposite walls coalesce to form full column is observed from the measured radial profile of the spectral line emission intensity from within the cathode space. The occurrence of this fully developed hollow cathode discharge is found to depend on the pressure of the working gas p, the discharge current I_A and the hollow cathode configuration. The results obtained agrees with those deduced from the optimum pressure range defined in the V_A versus p (I_A fixed) curves. HeI triplet and singlet lines are detected under most of the discharge conditions and hollow cathode configuration investigated but the singly charged ionic line HeII 468.57 nm is detected only at conditions under which the fully developed hollow cathode discharge is defined. The radial distribution of the ionic HeII line emission is indicative of the radial distribution of the high energy (~10^2 eV, close to the cathode fall potential) electron densities and is observed to peak at the axis. The total intensities of the HeI emission lines are found to be proportional to $I_A^{(0.8-1.2)}$ while that of the ionic HeII emission line is proportional to $I_A^{3.3}$. The width of the cathode dark space is deduced from the radial distribution profiles of the emission lines. From these, the average reduced electric field in the cathode dark space is also estimated.

I. INTRODUCTION

The hollow cathode was first described by Paschen [1] in 1916. Since then, its fundamental characteristics have been studied extensively. Basically, when two plane parallel cathodes are brought close enough their negative glows will coalesce. This is accompanied by an increase in the current density, by several orders of magnitude [2] at almost constant discharge potential, and enhanced emission intensity of the coalesced negative glow within the hollow cathode. This is said to be the hollow cathode effect. It is generally believed that the above are due to the efficient geometric confinement of ions, photons and metastable excited atoms that causes secondary electron emission from the cathode. Besides that, the effective trapping of the pendular electrons in the cavity due to the electric field distribution brings about enhanced ionization [2-8].

The hollow cathode can take many forms but higher plasma densities are achieved with cylindrical hollow cathode, making it an optimum choice for many applications. The geometric parameters of the cylindrical hollow cathode that can influence the discharge characteristics include its radius r (or half the separation distance in the case of a pair of plane-parallel cathodes) and length l. For hollow cathode discharge operation, the ratio of $l:r$ must not exceed approximately 14 [9]. The pressure of the filling gas is another dependent parameter and it is required that 1 torr-cm < $2pr$ < 10 torr-cm for rare gases, where r must not be less than the cathode dark space width d_k for a particular gas pressure [10].

It is the purpose of this work to obtain the radial profile of the spectral emission of HeI and HeII lines from the cylindrical hollow cathode, from which the dependence of a fully developed hollow cathode effect on the discharge conditions may be determined and compared to those deduced through other methods. The radial profile of the ionic line HeII 468.5nm gives information about the distribution of electron density within the hollow cathode. On integrating the emission intensity distribution over the cross-sectional plane of the cylindrical hollow cathode, the dependence of the total emission intensity on the discharge current I_A is studied. Besides that, the cathode dark space width d_k may also be measured and subsequently the average reduced field within the cathode dark space is estimated.

II. EXPERIMENTAL SETUP

The hollow cathode discharge configuration has been described in reference [11] whereas the experimental setup for measuring the optical emission from one end of the hollow cathode is shown in Fig. 1. The light emission from one end (with glass window) of the hollow cathode cylinder is imaged via a bi-convex quartz lens of focal length f = 5 cm. The image is allowed to fall on a PVC disc with a row of 1.1 mm diameter holes at intervals of 1.5 mm along a radial direction, in which the tip of a single core quartz fiber optic cable of diameter 1.0 mm may be inserted. The optical axis of the arrangement is along the hollow cathode axis and passes through the center of the PVC disc. It is sufficient to monitor the radial intensity

distribution of the hollow cathode along any chosen diameter as the radiation emitted is assumed to be symmetrical about the axis of the cylindrical hollow cathode.

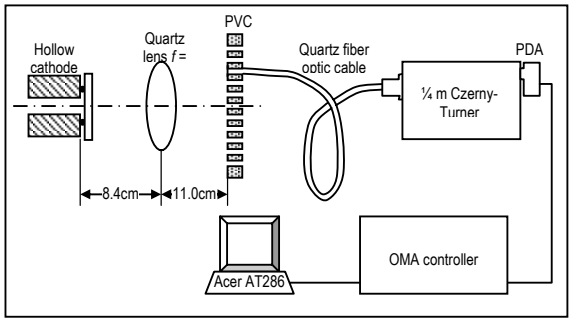

FIG. 1. Experimental setup for optical emission measurement.

The other end of the fiber optic cable is mounted onto the input slit of a ¼ m Czerny-Turner monochromator (model PTI 01-001) with a 1200 lines/mm grating blazed at 500 nm. The optimum slit width is found to be at 130 μm. A photodiode array (PDA) model 1453AC is mounted onto the output slit of the monochromator. This PDA is connected to the EG&G PARC's detector interface controller model 1461/88 and communicated to the computer via IEEE-488 GPIB.

The radial intensity distribution of the luminous glow in the cylindrical hollow cathode is measured for the HC6512 (diameter = 6.5 mm; length = 12 mm; l:r = 3.7) and HC1612 (diameter = 16 mm; length = 12 mm; l:r = 1.5) configuration. This ensures that the negative glow fills the whole length of the hollow cathode over the range of operating conditions studied (p = 0.5 mbar – 20 mbar; I_A = 2 mA – 40 mA) such that axial uniformity may be assumed. The spectral range obtained lies within the visible range of 350 nm – 750 nm. The radial emission profile of the smaller diameter hollow cathode HC6512 is measured at seven positions along a diameter of its image on the detection plane; whereas the HC1612 at fifteen positions.

As the radial emission intensity profiles take on different shapes at different operating conditions, it is more appropriate to consider the total radiation intensity from the hollow cathode and its dependence on these conditions. The total relative emission intensity is then obtained by integrating over the cross-sectional area of the hollow cathode assuming azimuthal symmetry.

III. RESULTS AND DISCUSSION

The wavelengths of the HeI and HeII lines measured in the present hollow cathode discharge setup are listed in Table I. The appearance and intensity of each line depend on the discharge conditions and hollow cathode configuration. Besides the HeI and HeII lines, H 656.28 nm and H 486.13 nm lines are also detected. This is due to the presence of water vapor (< 3 ppm) present in the purified He (99.999%) gas used. Although some sputtering occurs in the hollow cathode discharge as evident from the deposited film on the glass window, no spectral line relating to the elemental constituents of the cathode material is detected within the visible spectrum scanned.

Table I. Wavelengths (in nm) of the HeI and HeII lines identified from the spectrum measured for radiation emission from the hollow cathode discharge.

a. Helium I											
Triplet-triplet transition						Singlet-singlet transition					
$nd^3D - 2p^3P$		$ns^3S - 2p^3P$		$np^3P - 2s^3S$		$nd^1D - 2p^1P$		$ns^1S - 2p^1P$		$np^1P - 2s^1S$	
3d	587.56	*3s*	706.52	*3p*	388.86	*3d*	667.81	*3s*	728.13	*3p*	501.57
4d	447.15	*4s*	471.31			*4d*	492.19	*4s*	504.77	*4p*	396.47
5d	402.62					*5d*	438.79				
6d	381.96										
b. Helium II											
$nf^2F^0 - 3d^2D$											
4f	468.57										

Parameters which influence the radial profile of the glow intensity of the hollow cathode discharge include the discharge current I_A, helium pressure p and the hollow cathode configuration (especially its diameter). Different emission lines also exhibit their individual radial profiles. The dependences of the radial profiles on I_A and p at one of the strong emission lines (667.81 nm) in the HC6512 and HC1612 configurations are shown in

Figs. 2 and 3 respectively. The intensity of the radial profile increases with the discharge current I_A. At low pressure range, the profile exhibits a maximum at the center reminiscent of a bright central coalesced column of the negative glows from opposite cathode walls. As p increases, this bright column becomes annular in shape (the coalesced negative glow breaks up) which is shown as a dip in intensity at the center with two prominent maxima, one to the left and the other to the right. These maxima at the glow edges seem to move outwards as p is increased further.

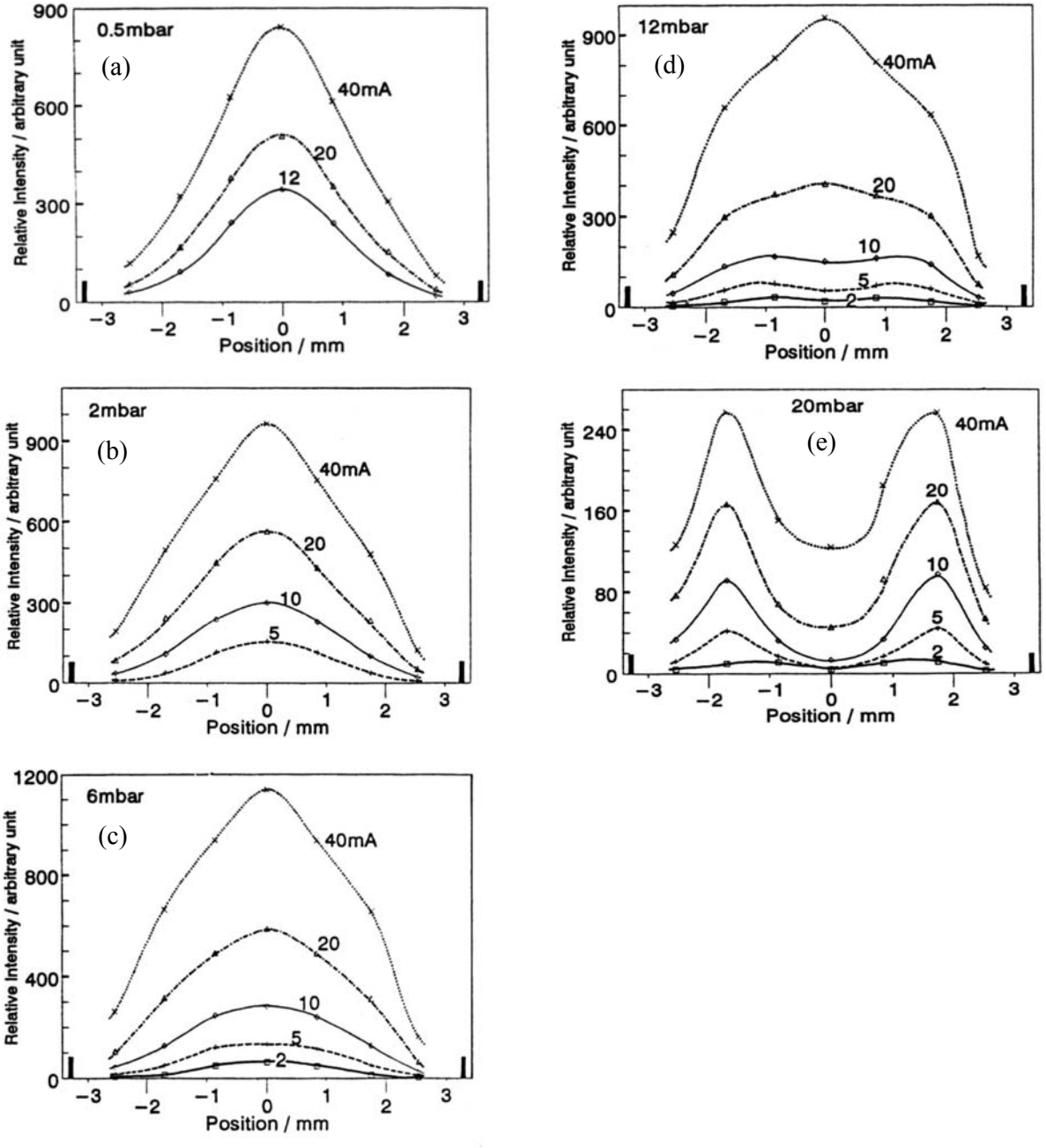

FIG. 2. Variation of the radial profile of the HeI 667.81 nm ($3d^1D - 2p^1P$) emission line intensity in the HC6512 configuration with discharge current I_A at helium pressures p of (a) 0.5 mbar; (b) 2 mbar; (c) 6 mbar; (d) 12 mbar and (e) 20 mbar.

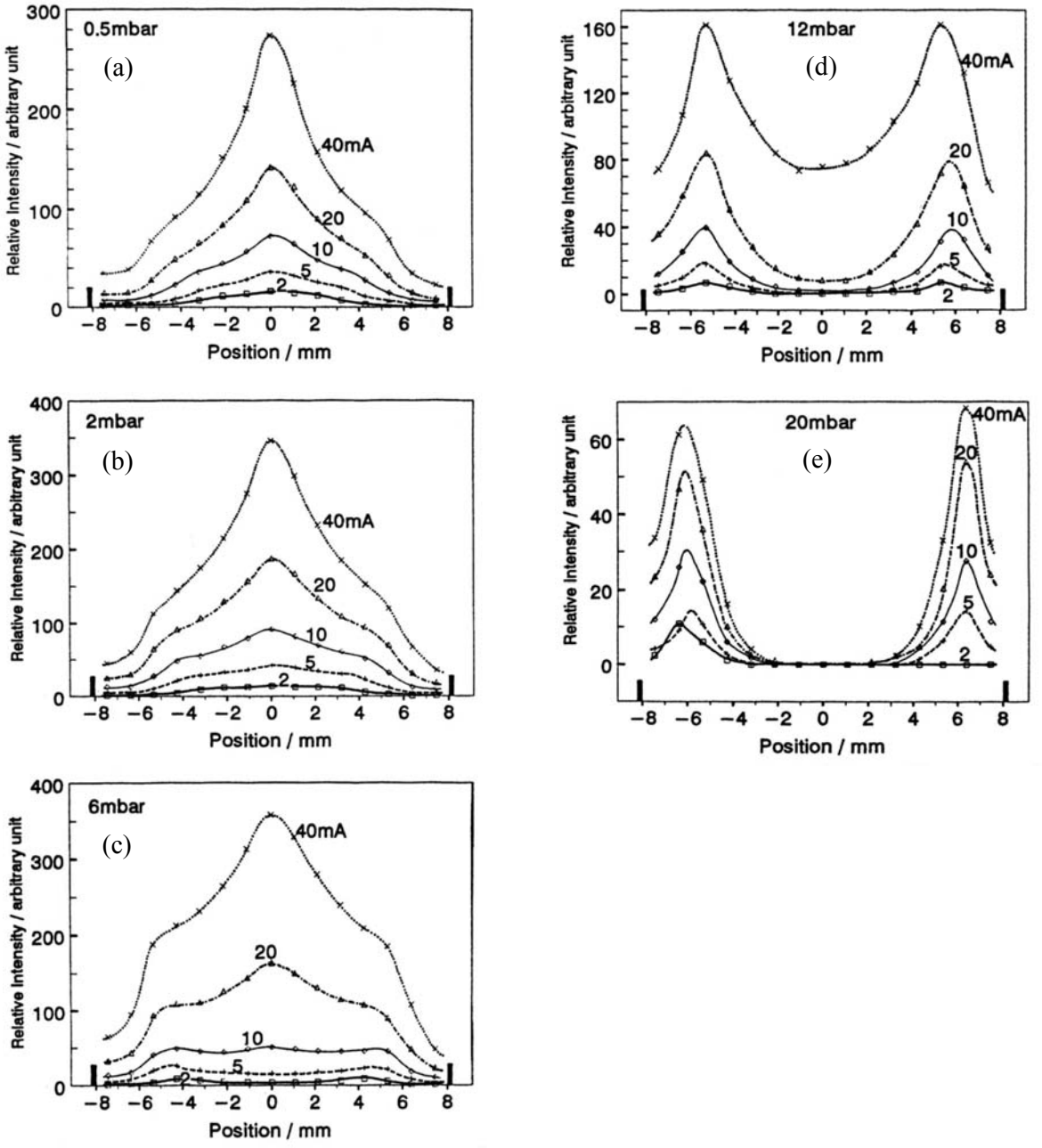

FIG. 3. Variation of the radial profile of the HeI 667.81 nm ($3d^1D - 2p^1P$) emission line intensity in the HC1612 configuration with the discharge current I_A at helium pressures p of (a) 0.5 mbar; (b) 2 mbar; (c) 6 mbar; (d) 12 mbar and (e) 20 mbar.

On closer examination of the radial emission profiles, those that exhibit a maximum at the center also hint on the presence of two maxima, one each to the left- and right- at the glow edges. These are more distinct in the HC1612 configuration. The ratio of the maximum at the center to the averaged maxima at the glow edges $I_{MAX\text{-}AXIS} : I_{MAX\text{-}EDGE}$ is shown in Fig. 4 as a function of p for fixed values of I_A. A ratio larger than unity represents a coalesced negative glow column at the center in which a fully developed hollow cathode discharge may be assumed. As the ratio dips below unity, the central bright coalesced negative glow column breaks up and the hollow cathode effect diminishes, reverting to a conventional planar cathode discharge. This transition

point occurs at p = 10 mbar for I_A = 10 mA in HC6512 and at p = 2.5 mbar for I_A = 2 mA in HC1612, moving to higher pressures as the current is increased. This behavior agrees with that of the upper limit of the optimum pressure range obtained from the plots of discharge voltage V_A versus pressure p at fixed discharge current I_A, in which the fully developed hollow cathode discharge is manifested by the region of positive gradient. Only the HeII 468.57 nm ($4f^2F^0$ – $3d^2D$) line from among the possible excitation states in the singly ionized helium atom is detected in the HC6512 configuration and its radial emission profile is shown in Fig. 5. The profile generally shows peak intensity at the center. It should be noted that these shapes may not be accurate as the overall intensity level is very low with poor resolution. The operating conditions in which this HeII line is discernable are at I_A = 40 mA for p = 0.5 – 12 mbar and at I_A = 20 mA for a comparatively smaller range of p = 6 – 12 mbar. In the hollow cathode of larger diameter HC1612, it is detected (low intensity) only at 40 mA, 6 mbar and at the center. The range of operating conditions under which this ionic HeII emission line is detected corresponds approximately to those of a fully developed hollow cathode discharge; the smaller diameter being more favorable than the larger one. The intensity profile may be taken as an image of the radial distribution of the concentration of the electron density of the very fast electrons toward the axis out of simple geometric reasons. The excitation functions of the atomic HeI lines generally peak at about 30 eV – 40 eV [12]. This means that an electron which may attain the full cathode fall potential of (200 – 400) eV (assuming that most of the discharge voltage V_A falls across the cathode dark space) can excite many atoms one after the other. In contrast, the excitation function of the ionic HeII line becomes appreciable at electron energies larger than 75 eV and peaks at around 200 eV [12] so that only unscattered electrons which have never undergone any collisions are able to excite these states. Initially these very fast electrons are directed toward the axis by the radial field in the cathode dark space. If they can keep this direction by not being scattered and then hit an atom, they could ionize and excite at the same time. The excited ions have short lifetimes and radiate immediately, their emission profile being a true picture of the density distribution of the exciting electron species [13]. Kuen et al. [13] have shown similar profile of the ionic HeII lines (468.5 nm and 320.3 nm) with a peak at the axis in a helium hollow cathode discharge (4 cm length, 2 cm diameter; l:r = 4) at 2.3 mbar and (10 – 25) mA. The accumulation of the very fast electrons at the axis is also evident from the numerical calculation of the distribution function of the electrons with the Monte Carlo method by Hashiguchi and Hasikuni [14] in a cylindrical hollow cathode of 1 cm diameter and 3.6 cm length (l:r = 7.2) at cathode fall potential of 300 V. It was also shown that the peak at the axis decreases with increasing gas pressure and these very fast electrons could hardly penetrate into the axis at p = 13 mbar. It is inferred that the fully developed hollow cathode discharge can sustain electrons of energy as high as the cathode fall potential.

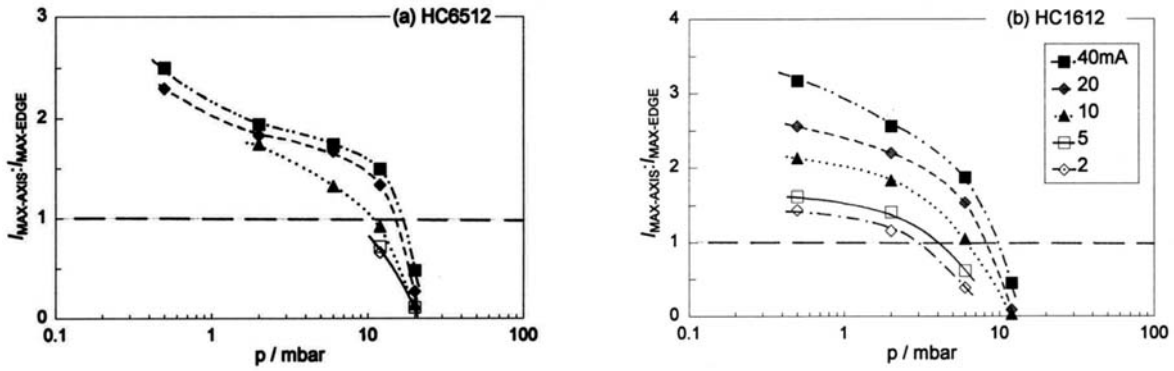

FIG. 4. The ratio of maximum intensity at the center to the averaged maxima intensities at the glow edge $I_{MAX-AXIS}$: $I_{MAX-EDGE}$ (deduced from the HeI 667.81 nm radial intensity profiles) is shown as a function of helium pressure p at various fixed discharge currents I_A for the (a) HC6512; and (b) HC1612 configurations.

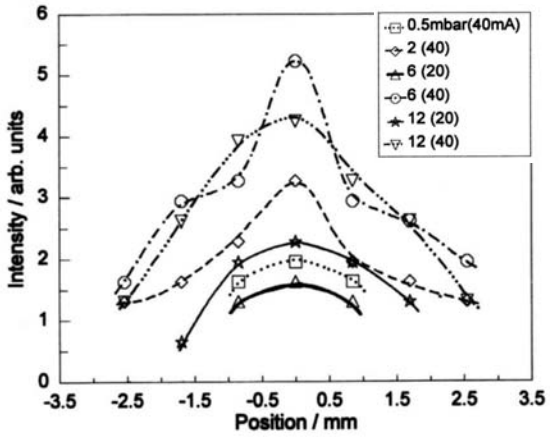

FIG. 5. Radial intensity profile of the HeII 486.515 nm line emission in the HC6512 configuration.

The integrated total intensity of the line emission from the glow in the hollow cathode discharge is shown in Fig. 6 to increase with discharge current I_A at fixed helium pressure p = 6 mbar. It is deduced that the total intensities of the line emission in the HeI spectrum are proportional to $I_A^{(0.8\ -\ 1.2)}$ while that of HeII line is proportional to $I_A^{3.3}$ in the HC6512 configuration. It is noted that the order of proportionality of the HeII line may be inaccurate as it is drawn from only two data points. The HeI emission lines from the HC1612 configuration shows a relation of total intensity $\propto I_A^{(0.6\ -\ 1.2)}$. These dependences are similar to those of neon emission lines from a Ne-Mo hollow cathode discharge (parallel plates of 4 × 4 cm^2; 0.4 cm separation; l:r = 20; p = 8 mbar) shown by Musha [15]. He also showed that the intensities of emission lines of Mo atoms vary nearly proportional to I_A^3. He then deduced that the Ne-Mo hollow cathode discharge was dominated by metal vapor of the cathode material as the total radiation was found to vary proportional to I_A^3. As sputtering of cathode material is due to energetic ions (most likely He^+ ions in the present setup, although it is known that sputtering yield in helium is very low), the deduced proportionality of the HeII line to the $I_A^{3.3}$ is reasonable. Some sputtering did occur as was confirmed from the Fe and Cr elements identified in the coating deposited on the glass window at one of the open end of the hollow cathode through the Energy-Dispersive X-ray Analysis (EDXA) spectrum. Fe and Cr are among the elemental constituents of the stainless steel hollow cathode material.

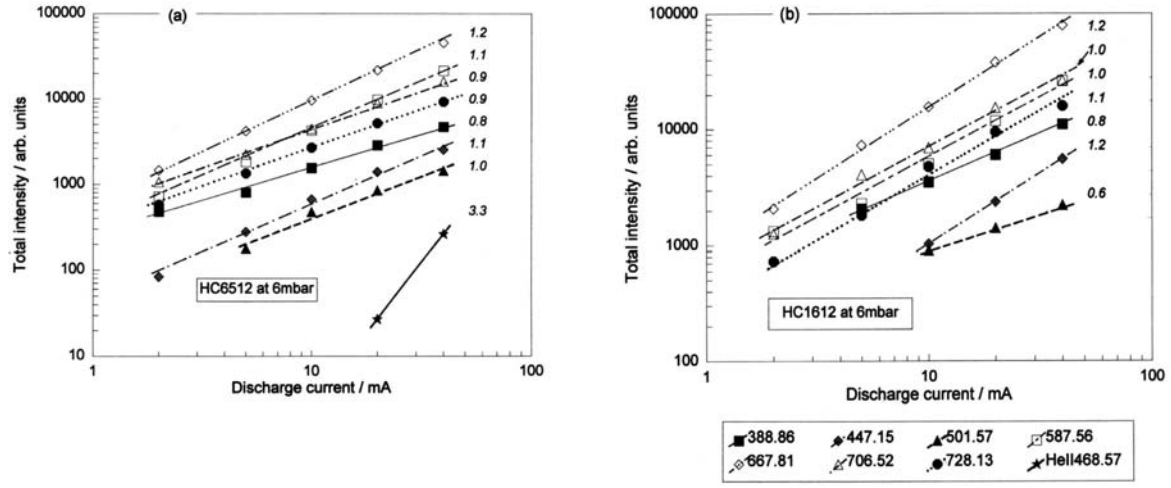

FIG. 6. The dependences of the total intensities of various HeI and HeII emission lines on the discharge current I_A at a fixed pressure of 6 mbar in the (a) HC6512 and (b) HC1612 configurations.

The cathode dark space width d_k (equal to the distance between the cathode surface to the boundary between the negative glow and the cathode dark space) may be deduced from the measured radial emission intensity profiles. The location of the boundary is taken to be at the point in which the gradient of the glow intensity is a maximum [16]. In the case of HC6512 in which the number of intensity detection points along the radial direction is small, the point at which half maximum intensity occurs is taken to be the boundary. From the radial profiles of the HeI emission lines of strong intensity, the variation of the cathode dark space width d_k (averaged over the left and right sides of the negative glow) with pressure at various discharge current

is obtained and shown in Fig. 7. At low I_A, d_k decreases with increasing p, being extremely steep in the hollow cathode of larger diameter (HC1612). As I_A is increased at fixed p, d_k generally gets narrower (especially at $p <$ 10 mbar). At high I_A and over the mid-pressure range which corresponds to the optimum pressure range (positive gradient) shown in Fig. 8, d_k is observed to remain almost constant. These agree with those reported by Kirichenko et al. [16] in a He-Ni hollow cathode discharge (length 20 cm, diameter 3 cm; l:r = 13.3). It is concluded that the width of the cathode dark space remains constant when the hollow cathode effect is fully developed in agreement to that which was reported by Little and von Engel [2].

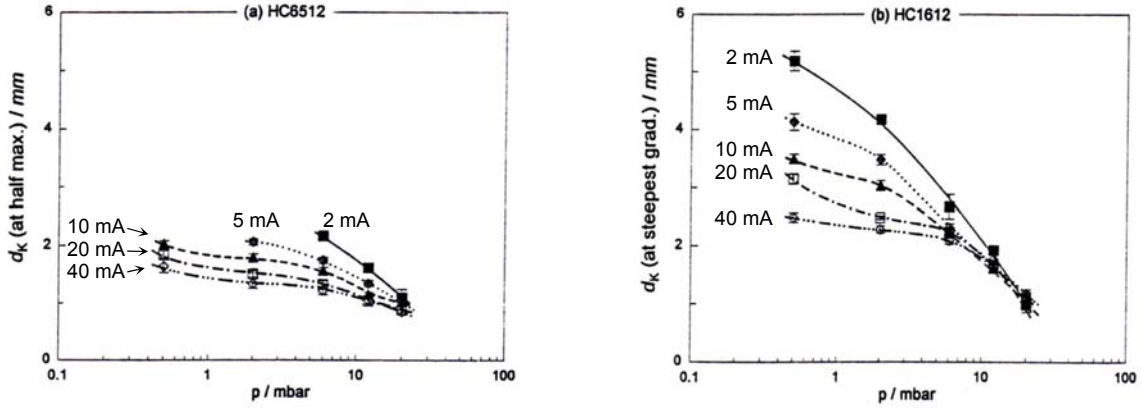

FIG. 7. Variation of the cathode dark space width d_k with pressure p for (a) HC6512 and (b) HC1612 configurations.

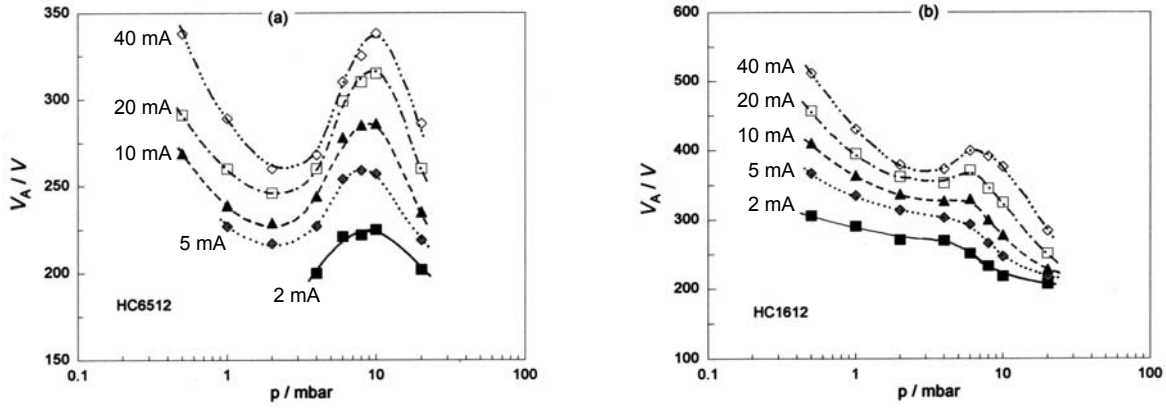

FIG. 8. The corresponding optimum pressure range depicted by region of positive gradient in the $V_A - p$ (at fixed I_A) curves for (a) HC6512 and (b) HC1612 configurations. (V_A is the anode or discharge voltage.)

It has been shown that the electric field falls linearly from the cathode towards the edge of the coalesced negative glow where the field is zero in a hollow cathode configuration [2, 17]. As most of the potential fall is across the cathode dark space, the average value of the electric field can be estimated from the ratio of the cathode fall potential V_k and the width of the cathode dark space d_k. It is assumed that $V_k \approx (V_A - 25)$ V; the difference of 25 V is the averaged difference between the measured plasma potential in the negative glow and the anode voltage V_A. In comparison, Kirichenko et al. [16] have shown V_k and V_A to differ by ≈ 20 V. It is seen from Fig. 9 that the estimated average value of the reduced field E/p in the cathode dark space is higher at lower pressure but higher current, thereby, resulting in the ions which traverse from the glow bombarding the cathode with higher attained energy. This leads to higher sputtering rate which explains the visually observed deposited coating on the glass window being more pronounced at lower pressure but higher current.

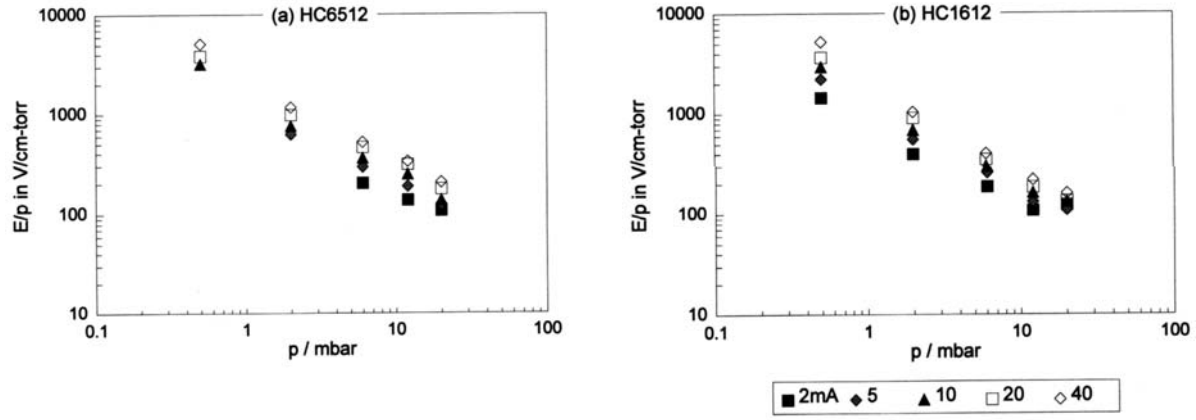

FIG. 9. Variation of the estimated reduced field *E/p* across the cathode dark space in the (a) HC6512 and (b) HC1612 configurations.

IV. CONCLUSION

The operating conditions in which a fully developed hollow cathode discharge occurs deduced from the radial emission intensity profiles (in which a coalesced full column of negative glow in the center of the hollow cathode is seen) correspond to those observed in the optimum pressure range defined by the positive gradient in the $V_A - p$ (at fixed I_A) curves. The ionic HeII 486.515 nm line emission is detected in the operating range consistent with a fully developed hollow cathode discharge and it indirect indicates the presence of very energetic electrons (possibly achieving full cathode fall potential, V_k eV). Its radial profile adumbrates the radial distribution of these fast electrons, which peaks at the axis. The total intensity of the atomic HeI lines is found to be proportional to $I_A^{(0.6-1.2)}$ while that of HeII line is proportional to $I_A^{3.3}$. These are in agreement with those observed by Musha [15]. The cathode dark space width d_k estimated from the radial emission profiles is almost constant under fully developed hollow cathode discharge operation consistent with those observed in by other researchers [2,16]. Increased sputtering observed to occur at low p and high I_A is facilitated by the relatively large reduced field *E/p* in the cathode dark space.

ACKNOWLEDGEMENT

The authors are grateful to the Ministry of Science, Technology and the Environment of Malaysia for supporting this work under the IRPA Program 4-07-04-40-05.

REFERENCES

[1] F. Paschen, Ann. Phys., **50**, 901 (1916).
[2] P. F. Little and A. von Engel, Proc. Roy. Soc., **A224**, 209 (1954).
[3] A. Güntherschulze, Z. Physik, **19**, 313 (1923).
[4] A. von Lompe, R. Seeliger and E. Wolter, Ann. Physic. **36** (5), 9 (1939).
[5] M. J. Druyvesteyn and F. M. Penning, Rev. Mod. Phys., **12**, 87 (1940).
[6] E. Badareu and I. Popescu, J. Electron. Control, 1st series, **4**, 503 (1958).
[7] K. G. Hernqvist, RCA Review, **19**, 35 (1958).
[8] A. D. White, J. Appl. Phys., **30** (5), 711 (1959).
[9] C. S. Willet, *Introduction to Gas Lasers: Population Inversion Mechanisms*, Pergamon Press, New York (1974), p. 79.
[10] J. W.Gewartowski and H. A. Watson, *Principles of electron tubes*, Van Nostrand, Princeton, New Jersey (1965), p. 56.
[11] O. H. Chin and C. S. Wong, J. Fiz. Mal., **23** (1-4), 54-59 (2002).
[12] L.J. Kieffer, Atomic Data, **1**, 121 (1969).
[13] I. Kuen, F. Howorka and H. Störi, Phys. Rev. A, **23** (2), 829 (1981).
[14] S. Hashiguchi and M. Hasikuni, Jpn. J. Appl. Phys., **27** (6), 1010 (1988).
[15] T. Musha, J. Phys. Soc. Jpn., **17**, 1440 and 1447 (1962).
[16] V. I. Kirichenko, V. M. Tkachenko and V. B. Tyutyunnik, Sov. Phys. - Techn. Phys., **21** (9), 1080 (1976)
[17] K. Takiyama, T. Usui, Y. Kamiura, T. Fujita, T. Oda and K. Kawasaki, Jpn. J. Appl. Phys., **25** (6), L455 (1986)